Available online at www.sciencedirect.com
ScienceDirect
Journal of the European Ceramic Society 28 (2008) 2117–2127
www.elsevier.com/locate/jeurceramsoc

Experimental and FEM-supported investigation of wet ceramic clay extrusion for the determination of stress distributions on the applied tools' surfaces

K.-D. Bouzakis [a,*], K. Efstathiou [a], G. Paradisiadis [b], A. Tsouknidas [a]

[a] *Laboratory for Machine Tools and Manufacturing Engineering, Mechanical Engineering Department, Aristoteles University of Thessaloniki, GR-54124 Thessaloniki, Greece*
[b] *Department of Vehicle Technology, Technological Educational Institution of Thessaloniki, Greece*

Received 10 October 2007; received in revised form 13 February 2008; accepted 29 February 2008
Available online 2 May 2008

Abstract

Aiming at assessing the stress distribution on the surface of a die mandrel during the extrusion of ceramic products, the flow of wet ground clay was simulated both in a ram extrusion device and by a FEM-based model, considering the von Mises criterion for the flow stress, the associative flow rule and the rigid–viscoplastic constitutive equation. The friction between clay and die is approached by the Tresca boundary condition, which proves a more realistic approach than the Coulomb friction law for the contact conditions between a plastically deforming material and a rigid surface. The Tresca friction factor and the material parameters of the constitutive model are determined through comparison of experimental and theoretical results. The distributions of clay sliding velocity and normal and frictional stress on the mandrel surface are then assessed through the numerical simulation model. It is found that no sticking areas appear on the mandrel surface.

Keywords: Extrusion; Plasticity; Clays; Friction; Stress distribution

1. Introduction

The calculation of the flow of wet ground clay during the extrusion of ceramic products (bricks or tiles) is necessary for the assessment of the loads occurring on the extrusion dies and their resulting wear. The applied types of clay can exhibit considerable variation in their chemical composition and grain size distribution and consequently in their mechanical properties. After the removal of foreign bodies and the downsizing of the bigger grains in a drum crusher, water in proportion of about 15% on the weight of the dry clay is added. The resulting wet clay is a paste-like, macroscopically homogenous mixture with the ability of retaining its shape and sustaining small tensile stresses, behaving practically as a soft solid.

The behaviour of such paste-like materials in extrusion processes, where the imposed strains are orders of magnitude larger than the elastic strains, is well described by the rigid–viscoplastic constitutive model.[1–5] However, there are few comparable experimental data on the material parameters of the constitutive model, even less so for wet ground clay. Furthermore, there appears often considerable disagreement between such data provided by different authors, not least as a result of different boundary conditions used to describe the friction between clay and die, which due to the relatively high size of the friction force in every practical application or experimental procedure are of crucial importance for the numerical simulation results.[1,2,4–6]

In order to determine the loadings of the die mandrels' surface thin hard coatings during brick extrusion an experimental and theoretical simulation has been carried out. The flow of the wet clay around a die mandrel is simulated in a ram extruder and the measured force–displacement curve is compared with the results of a finite element simulation model based on the von Mises criterion for the flow stress, the rigid–viscoplastic constitutive model and the Tresca boundary condition. The values of the constitutive model parameters and the Tresca friction factor for a certain type of clay used in a production plant are obtained by fitting the numerical results with the experimental data. The

* Corresponding author. Tel.: +30 2310 996079; fax: +30 2310 996059.
E-mail address: bouzakis@eng.auth.gr (K.-D. Bouzakis).

0955-2219/$ – see front matter © 2008 Elsevier Ltd. All rights reserved.
doi:10.1016/j.jeurceramsoc.2008.02.027

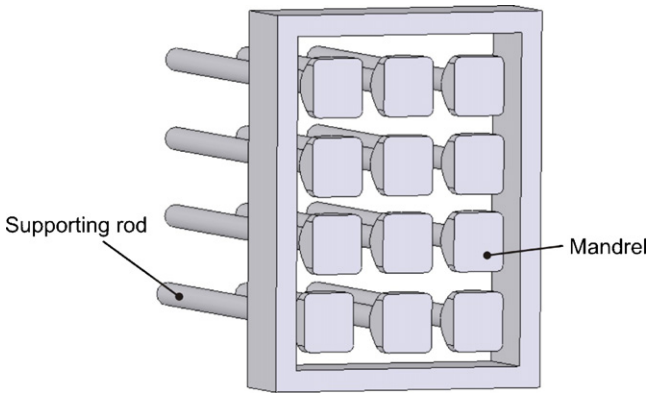

Fig. 1. Schematic presentation of a section set of a brick extrusion die.

stress and clay velocity distributions on the surface of the mandrel as well as the flow pattern of the clay in the vicinity of the mandrel as assessed by the FEM simulation model are presented and discussed.

2. Experimental procedure and results

A characteristic section set of a brick extrusion die is depicted in Fig. 1. The set consists of a frame and several supporting rods onto which the die mandrels are screwed. The clay is being thrust through the die mandrels by clay driving forward rotating screw, producing a continuous column of the cross-section of the brick, which then passes through an automatic cutter. A die usually comprises four to six brick section sets. The frame and the rods are made of steel, whereas the mandrels, which undergo the severest tribological strain and exhibit the highest wear, are usually made of a friction resistant material, such as of hardened steel, cemented carbide or even ceramics. Since recent time PVD or CVD coatings contribute to a significant wear behaviour improvement of the applied mandrel materials.

Wet clay, as used in an extrusion press for brick production, was applied in the trials. Its main physical, chemical and mechanical properties are shown in Table 1.

Table 1
Physical, chemical and mechanical properties of the applied clay

Dry clay	
Chemical composition (% by weight)	
SiO_2	66.00
Al_2O_3	15.10
Fe_2O_3	5.00
CaO	2.25
MgO	1.67
K_2O	2.30
Na_2O	1.22
L.O.I.	6.42
Total	99.96
Grain size distribution (% by weight)	
<0.05 mm	60
0.05/0.15 mm	20
>0.15 mm	20

Wet clay: water content, 13.5% by weight; specific density, 1.950 kg/m^3.

The yield stress of paste-like materials can be determined either through the rheological calculation of an orifice or a squeeze film flow,[3,7] or through a compression test.[8,9] Both methods involve considerable inaccuracy due to simplification assumptions necessary for the calculation of the rheological flow, or to the difficulty to determine clearly the beginning of the plastic flow in the case of a compression test. As the applied wet clay exhibited a sufficiently clear beginning of plastic flow in compression tests, its yield stress could be determined through an unconfined compression test as 0.102 MPa, in the range of values presented in Refs. [7–9].

As shown in Fig. 2, the experimental device consists of a rectangular compression chamber with a cemented carbide die mandrel coated with a 10-μm thick diamond coating, fixed at its outlet. The chamber is filled with a prescribed quantity of wet clay, which is then extruded by a piston through the gap between mandrel and chamber. The geometry of the coated die mandrel is also shown in the figure. The short cylindrical shaft on the top of the mandrel simulates its holding rod and contributes to the development of similar clay flow conditions as in the brick extrusion die. The internal cross-section of the compression chamber is 32 mm × 34 mm, so as to reproduce the dimensions of the gap between the mandrels of the actual die.

The experimental set up to monitor various parameters during the clay extrusion is shown in Fig. 3. The piston is operated by a pneumatic cylinder. A control unit monitors and records the progress of piston force and piston displacement. The force applied by the piston is adjusted through a pressure regulator, while its speed is controlled by a strangulation valve on the upper part of the pneumatic cylinder. The wet clay is first pressed by the piston against a pad at the outlet of the compression chamber to ensure a continuous mass and release it from possible air enclosures. The piston then moves back to its starting position at the top of the chamber, the pad is removed and the clay is extruded by the piston, producing a single hollow column.

Two trials with different mean piston speeds of 46.5 mm/s and 235 mm/s were conducted, using the same quantity of wet clay. The measured curves of piston speed and piston force against piston displacement are shown in Fig. 4a and b, respectively. Starting at the top end of the chamber the piston accelerates until it contacts the mass of clay, where it decelerates sharply, while the piston force rises correspondingly as the extrusion begins. During the extrusion, in the range from 118 mm to 183 mm of the piston stroke, the piston force declines due to the decreasing friction between clay and chamber, causing a slight and steady increase of the piston speed. The comparison of the measured force curves with those obtained from the following numerical simulation was accomplished for the section of the piston stroke between 132 mm and 166 mm, as shown in Fig. 4a and b, where their slope is practically stabilized and not affected by the inertial factors acting in the beginning and the end of the extrusion range. As in this region the deviation of the actual piston speed from its mean value is less than 3% in both trials, a constant speed equal to the measured mean speed was assumed in the numerical simulation.

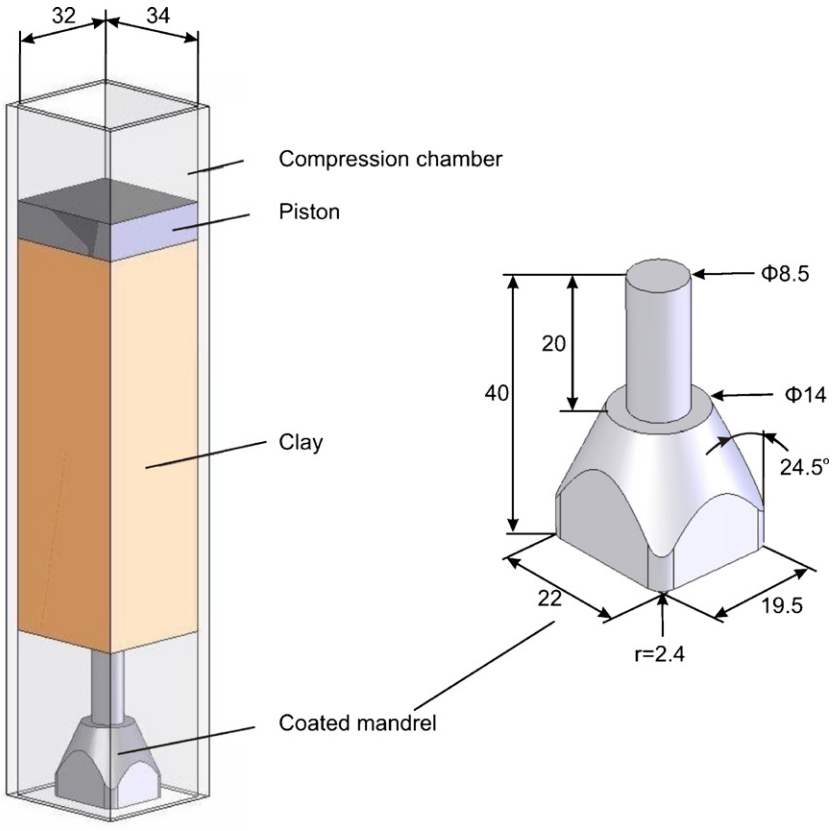

Fig. 2. Concept of experimental device and geometry of coated die mandrel.

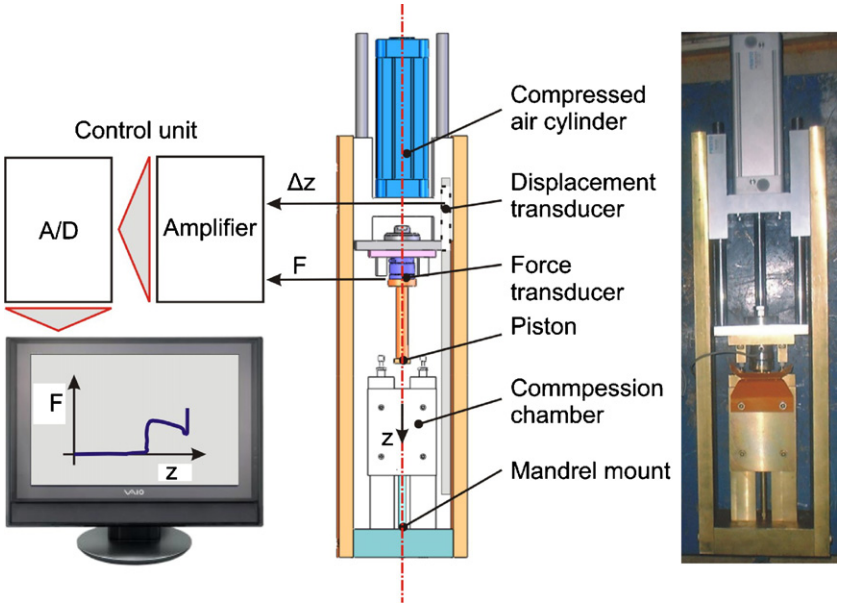

Fig. 3. Schematic representation and photo of the experimental device.

3. The developed FEM-supported simulation model

A numerical simulation model was developed to predict the force–displacement curves obtained from the trials. As the stresses applied on the clay are orders of magnitude higher than its yield stress of 0.102 MPa – at the end of the considered stroke section during the low speed (46.5 mm/s) trial, where the piston force is lowest, the pressure exerted by the piston on the clay is 2000 N/1088 mm^2 = 1.84 MPa –, it can be safely assumed that the entire mass of the clay is in a state of plastic deformation. Under such circumstances the elastic components of the strains are negligible and the strain rates are considered as plastic.

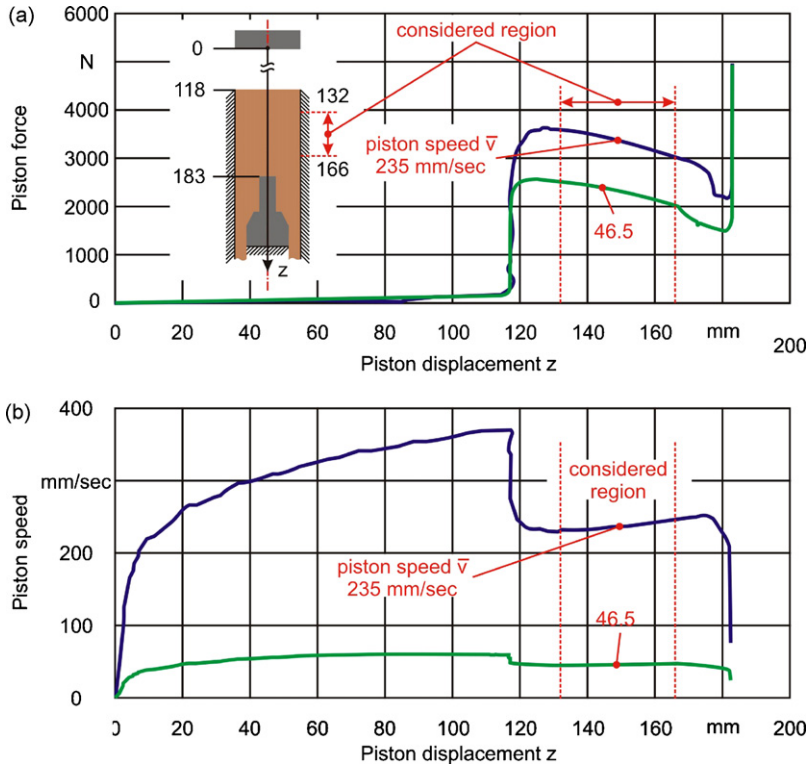

Fig. 4. Piston force and piston speed vs. piston displacement for mean piston speeds of 46.5 mm/s and 235 mm/s.

The wet clay, a highly concentrated dispersion of interactive particles in a continuous liquid phase (water), is assumed to be an isotropic material which follows the associative flow rule and the von Mises yield criterion,[4,5,10] so that under plastic flow, in a Cartesian coordinate systems x, y and z:

$$\dot{\varphi}_{ij} = \lambda s_{ij} \quad \text{and} \tag{1}$$

$$\lambda = \lambda(\sigma_{\text{fl}}) \tag{2}$$

where $\dot{\varphi}_{ij}$ are the strain rates and s_{ij} is the respective deviatoric stresses:

$$s_{ij} = \sigma_{ij} = \tfrac{1}{3}(\sigma_x + \sigma_y + \sigma_z) \quad \text{if } i = j, \quad s_{ij} = \sigma_{ij} \quad \text{if } i \neq j \tag{3}$$

and the flow stress σ_{fl} is the von Mises equivalent stress:

$$\sigma_{\text{fl}} = \sqrt{\frac{3}{2}(s_{xx}^2 + s_{yy}^2 + s_{zz}^2)} \tag{4}$$

The flow rate $\dot{\varphi}_{\text{fl}}$ under uniaxial stress σ_{fl} is obtained by applying Eq. (1) for the uniaxial stress condition and substituting σ_{fl} with Eq. (4):

$$\dot{\varphi}_{\text{fl}} = \lambda \frac{2}{3}\sigma_{\text{fl}} = \sqrt{\frac{2}{3}(\dot{\varphi}_{xx}^2 + \dot{\varphi}_{yy}^2 + \dot{\varphi}_{zz}^2)} \tag{5}$$

The shear flow stress τ_{fl} is obtained from the von Mises criterion as

$$\tau_{\text{fl}} = \frac{\sigma_{\text{fl}}}{\sqrt{3}} \tag{6}$$

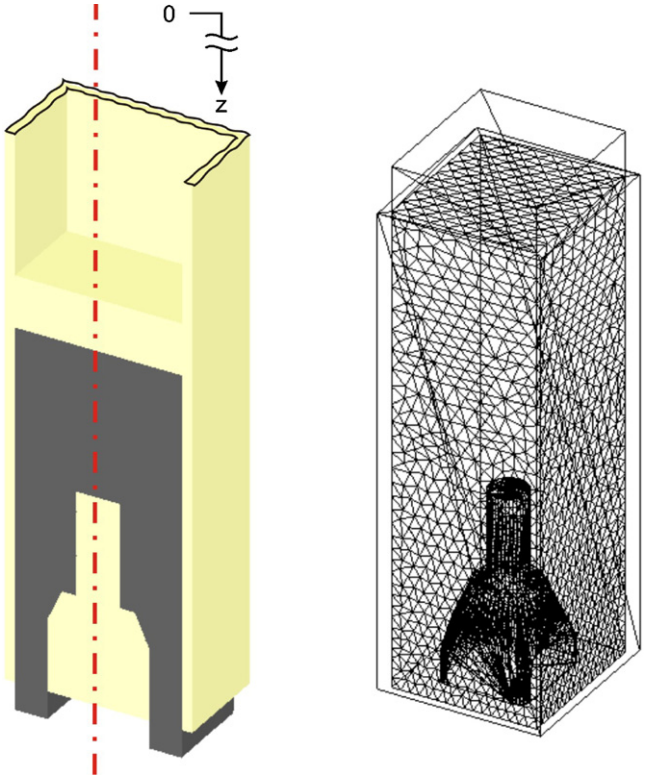

Fig. 5. Geometry of the numerical simulation model and initial finite element discretization of the clay.

The shear flow rate $\dot{\gamma}_{fl}$, i.e. the shear rate under pure shear stress τ_{fl}, results by applying Eq. (1) for pure shear:

$$\dot{\gamma}_{fl} = 2\lambda\tau_{fl} = 2\lambda\frac{\sigma_{fl}}{\sqrt{3}} = \sqrt{3}\dot{\varphi}_{fl} \tag{7}$$

The hardening behaviour of the clay is assumed to follow the Herschel–Bulkley relationship,[1,3–5] with the shear flow stress τ_{fl} a function of the shear flow rate $\dot{\gamma}_{fl}$:

$$\tau_{fl} = \tau_0 + K\dot{\gamma}_{fl}^n \tag{8}$$

where τ_0 is the shear yield stress, K the shear plastic flow consistency and n is the flow exponent of the clay.

Substituting τ_{fl} and $\dot{\gamma}_{fl}$ from Eqs. (6) and (7) and $\sigma_0/\sqrt{3}$ for τ_0 in Eq. (8), where σ_0 is the yield stress of the material, results in the Herschel–Bulkley relationship in uniaxial form:

$$\sigma_{fl} = \sigma_0 + k\dot{\phi}_{fl}^n \tag{9}$$

where

$$k = 3^{(n+1)/2}K \tag{10}$$

is the plastic flow consistency of the wet clay.

Since the temperature of the wet clay during the extrusion process remains approximately stable at about 40–50 °C, the characteristic material parameters k and n can be regarded as constant.

In the theoretical model the piston, the chamber and the mandrel are considered as rigid surfaces. The piston moves with a constant speed equal to the mean speed measured at the respective trial. For a material under plastic deformation in contact with a rigid surface, the Coulomb friction law,[1,2,7] according to which the maximum friction stress $\tau_{f,max}$ is proportional to the normal pressure p between the contacting bodies ($\tau_{f,max} = \mu p$), does not seem appropriate, as it assumes an actual contact surface proportional to the normal pressure p, which is not realistic for a plastically deforming material. Furthermore, as the decrease of the piston force with the descent of the piston is almost exclusively due to the reduction of the friction force between clay and chamber – the force on the mandrel remaining approximately constant because of the practically unchanging flow conditions around it –, the almost linear decrease of the measured piston force in the considered stroke section implies that the distribution of friction stress there does not vary significantly along the piston stroke. The Coulomb law instead, due to the decreasing normal pressure along the chamber wall, would result in a friction stress decreasing in proportion to the normal pressure and thus in a concave piston force curve. The nearly linear decrease of the piston force is thus an indication of the applicability of the Tresca friction law,[1,4–6,11] which assumes that the maximum

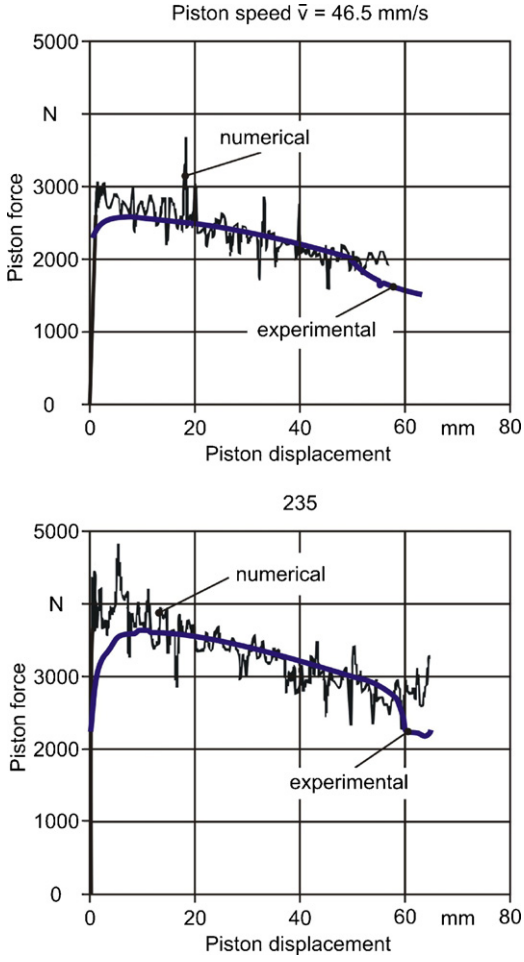

Fig. 6. Comparison between experimental and FEM—calculation results.

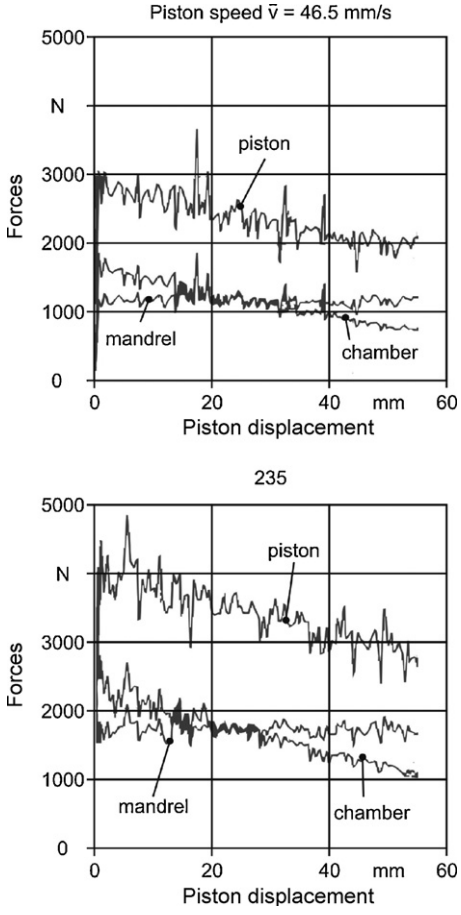

Fig. 7. Piston, chamber and mandrel forces against piston displacement at various piston speeds.

friction stress is a function of the shear flow stress τ_{fl} of the material at the considered point, independent of the normal pressure on the contact surface:

$$\tau_{f,max} = m\tau_{fl} \quad (11)$$

where m is a constant friction factor.

Indeed, since the flow of the clay along the considered region, where it is not influenced by the presence of the mandrel, does not change significantly, the strain rate distribution remains also practically unchanged. According to the Tresca friction law Eq. (11) and the constitutive Eq. (8), this results in a constant friction stress distribution along the piston stroke and thus to a linearly decreasing piston force.

As a result of the Tresca friction law the material should stick or slide on any point on the wall depending on whether the friction stress there is lower than or equal to the maximum value of the friction stress Eq. (11), respectively.

4. Assessment of the clay deformation parameters through comparison of experimental and numerical results

The numerical analysis was implemented with the use of the DEFORM finite element program for forming processes.[12] The geometry of the model, built with the SOLIDWORKS solid modeler,[13] and the finite element discretization of the wet clay billet with four-node tetrahedral solid elements at the beginning of the simulation are shown in Fig. 5. The element mesh is generated automatically by the AMG feature of DEFORM, providing for higher density in regions of high curvature or steep strain rate gradient. The mesh is maintained through successive steps of the clay deformation until serious distortions due to the large plastic deformations render it inefficient and a new mesh is automatically generated. The volume compensation feature of DEFORM was activated to maintain a constant material volume at remeshing, while the constant shear friction option was used to apply a common Tresca friction factor between the plastically deforming clay and the rigid surfaces of piston, chamber and mandrel.

There are few comparable estimates available for the unknown values of the three parameters of the numerical simulation model, namely the plastic flow consistency k, the flow exponent n and the Tresca friction factor m, referring mostly to materials such as plasticine or alumina paste,[1,2,5,7] but not to wet clay as used in the production of ceramic products. Since these data are not applicable to the wet clay, the values of the material parameters k, n and m were determined as the set of values for which the numerical simulation yielded the best fit with the experimentally obtained piston force curves. This was achieved by each time assuming a value for the Tresca friction factor m and then systematically varying the values of the parameters k and n until the numerical simulation for the higher piston velocity of 235 mm/s yielded the best agreement with the measured piston force curve. As both the experimental and calculated piston force curves are almost linear, the sum of the absolute differences between the measured and the calculated piston force values at the beginning and the end of the considered region (Fig. 4a and b) was used as fitting criterion. It was found that for each assumed values of m between 0.3 and 0.85 it was possible to find a unique set of k and n values for which the sum of the absolute differences between the measured and the calculated piston force values at the limits of the section of comparison was less than 2% of the sum of the measured piston force values there (3585 N and 3010 N, respectively). Values of m outside this range led to no satisfactory solution. Each set of m, k and n values obtained this way was then applied to the calculation of the piston force curve for the lower piston velocity of 46.5 mm/s, under the same fitting criterion—that the sum of the absolute differences between the measured (2505 N and 2005 N) and calculated piston force values at the limits of the considered region should be less than 2% of the sum of the measured piston force values there. In this way the combination of values of $m = 0.46$, $k = 0.37\ \text{MPa s}^{-n}$ and $n = 0.25$ was determined to yield the best agreement with the experimental results for both piston speeds. Thus the constitutive Eq. (9) for the wet clay under complete plastic deformation, as in the case of the extrusion of ceramic products, takes the form:

$$\sigma_{fl} = 0.102\ \text{MPa} + 0.37\ \text{MPa s}^{0.25}\dot{\varphi}_{fl}^{0.25} \quad (12)$$

and the Tresca friction factor between wet clay and die mandrel is determined as $m = 0.46$.

The comparison between the experimentally and the numerically obtained piston force curves is shown in Fig. 6. The fluctuation appearing in the calculated curves is due to the iteration procedures of the FEM solver and does not affect their actual course. The curve for the lower piston speed is predicted with nearly complete accuracy, whereas for the higher piston speed the numerical model yields a slightly steeper curve. Nevertheless the accuracy of the numerical model is deemed satisfactory, as the deviation between experimental and theoretical values does not exceed 2% for both piston speeds.

5. Determination of the mandrel surface loadings

The variation of the piston, chamber and mandrel forces along the piston stroke for the lower and higher tested mean piston speeds of 46.5 mm/s and 235 mm/s, respectively is shown in Fig. 7. The piston force is equal to the sum of the friction force on the chamber and the force on the mandrel. The force on the mandrel remains practically constant, attesting that the flow around it remains stable during the descent of the piston. It is clear that the value of the Tresca friction factor m is crucial for the theoretical simulation results, as the friction between clay and chamber makes up about half the piston force (the friction on the mandrel surface being also a substantial part of the force on the mandrel, as discussed later).

In a Cartesian coordinate system where the x and y axes lie in the directions of the longer (34 mm) and shorter (32 mm) sides of the chamber cross-section, respectively and the z-axis in the direction of the piston stroke, the calculated distributions of velocity in the z-direction, equivalent strain rate and equivalent (flow) stress on the contact surface of the clay with the

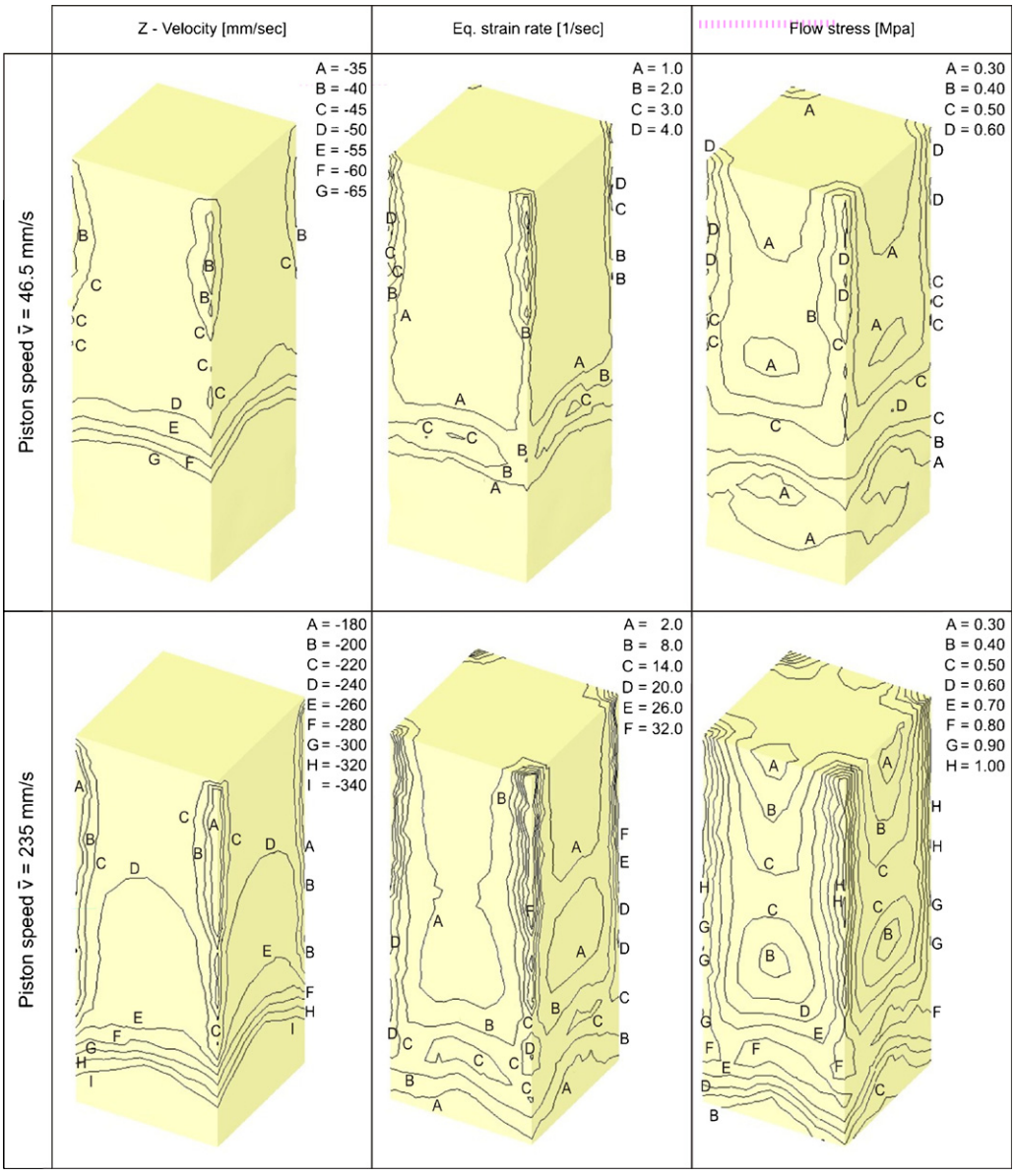

Fig. 8. Z–velocity, equivalent strain rate and flow stress distribution on the chamber wall at various piston speeds.

chamber and the piston, for a position of the piston approximately 155 mm from its starting position, are given in Fig. 8 for the lower and higher piston speed. Comparison with the results for other positions of the piston along its stroke has confirmed that the flow pattern of the clay around the mandrel remains virtually unchanged with the descent of the piston.

As seen in the velocity distributions, there are nowhere sticking areas, even at very low velocities, in accordance to experimental observation in Ref. [14]. In the upper part of the chamber, where the flow is not significantly affected by the presence of the mandrel, the bulk of the clay moves with roughly the speed of the descending piston—with the exception of small areas in the corners of the chamber, where there is a reduction in the vertical velocity of the clay of up to 30% for both piston speeds, as a result of higher friction there. Because of this deceleration, the clay flows from the corner areas towards the middle of the chamber, however its horizontal velocity gets considerable only very close to the corners, so that in almost the whole mass of the clay the horizontal (x and y) components of the velocity are practically negligible in comparison to the vertical (z) component. As the flow accelerates towards the narrower outflow cross-section, the strain rate and therefore the friction on the contact surfaces rise considerably. The outflow velocity profile is quite uniform though, both in the directions across the gap and along the wall, due to the relatively low impact of the friction stresses against that of the high value of the plastic flow consistency k.

For sliding contact, the value of the friction stress τ_f is calculated from Eqs. (6) and (11), for $m = 0.46$, as

$$\tau_f = \frac{m}{\sqrt{3}}\sigma_{fl} = 0.266\sigma_{fl} \tag{13}$$

Apart from the corner areas, where the horizontal component of the friction stress is considerable as a consequence of the

horizontal flow there, the friction stress on the wall is almost vertically directed. The highest values appear in the corner areas (0.26 MPa for the higher piston speed, for an equivalent strain rate of 30 s^{-1}) and to a lesser degree across the upper edges of the vertical sides of the mandrel (0.21 MPa), where the strain rate, and thus the flow stress, is highest.

Of particular interest for the examination of the mandrels' wear in a further stage of this investigation are the calculated distributions of clay sliding velocity, equivalent strain rate, friction stress and normal pressure on the die mandrel surface, which are presented in Figs. 9 and 10 for the lower and higher piston speed, respectively.

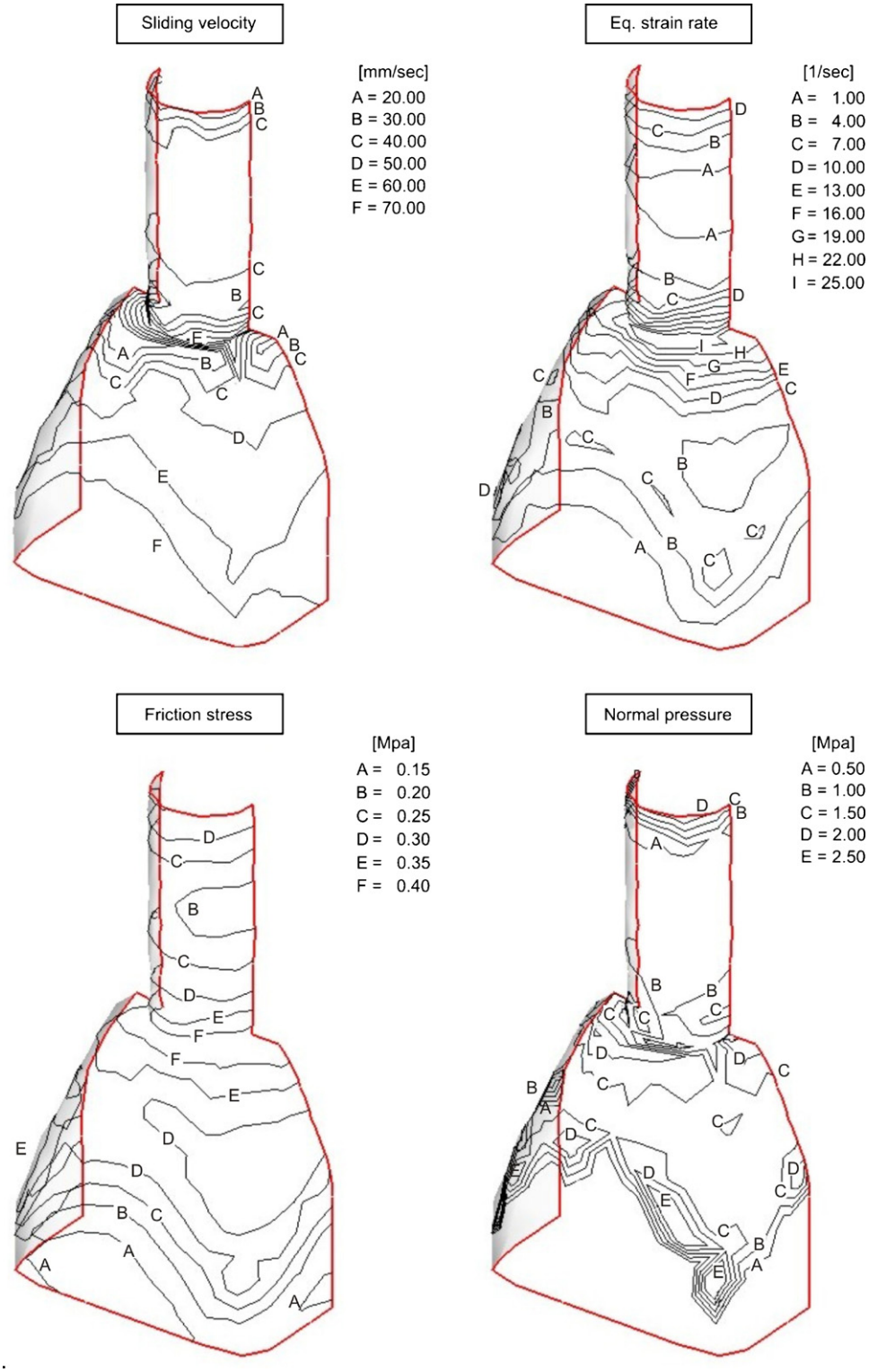

Fig. 9. Sliding velocity, equivalent strain rate, friction stress and normal pressure distribution on the surface of the die mandrel for a piston speed of 46.5 mm/s.

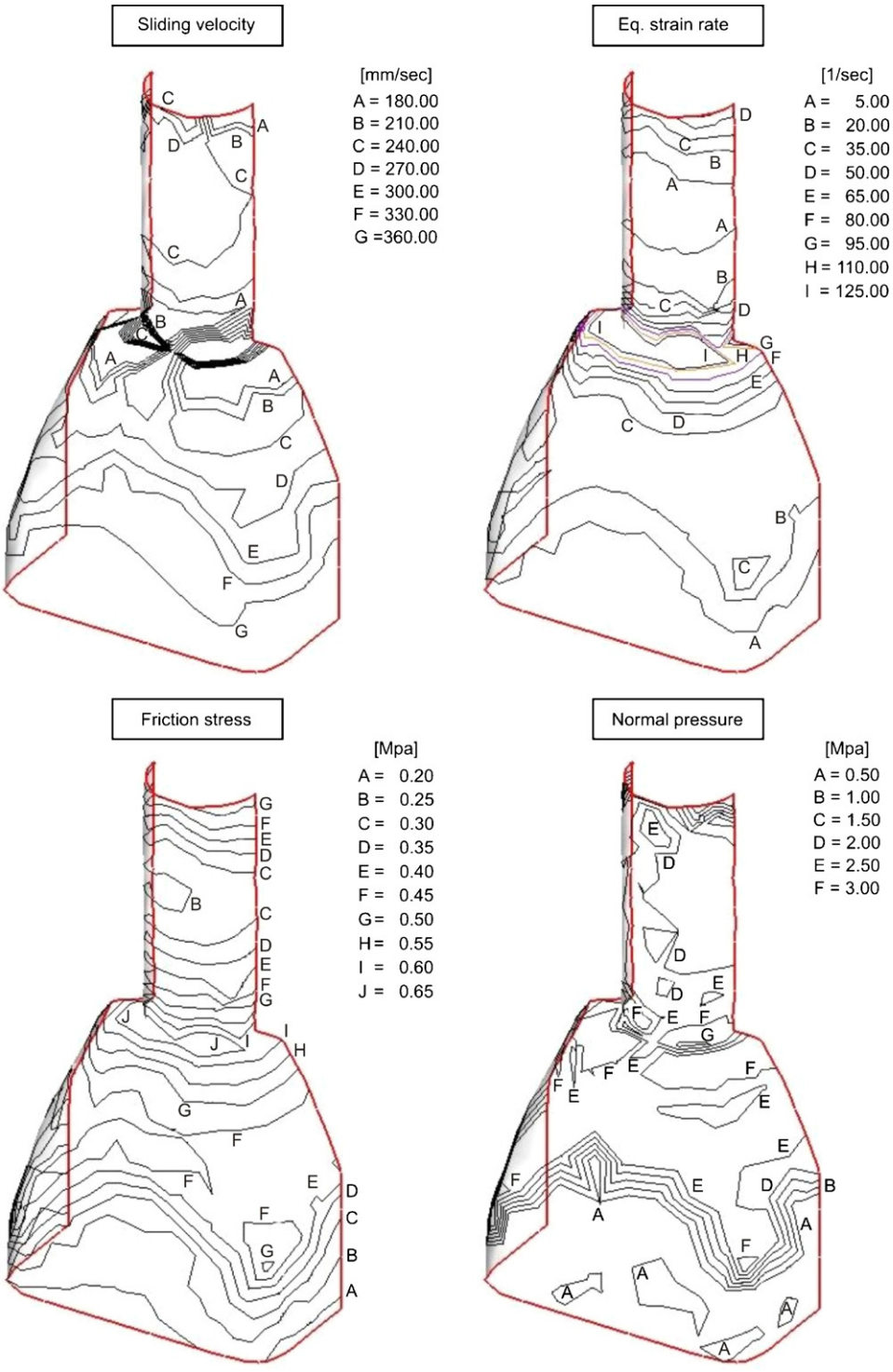

Fig. 10. Sliding velocity, equivalent strain rate, friction stress and normal pressure distribution on the surface of the die mandrel for a piston speed of 235 mm/s.

After acquiring a high sliding velocity by the junction of shaft and mandrel the clay decelerates on the upper horizontal surface of the mandrel and then accelerates on the inclined surface, until it almost reaches the outflow velocity at the edges of the vertical sides. The strain rate and accordingly the friction stress are highest on the horizontal surface of the mandrel close to the shaft (about 125 s^{-1} and 0.65 MPa, respectively, for the higher piston speed) and then decrease gradually towards the outlet. Normal pressure is also high on the horizontal surface of the mandrel, retaining high values on the inclined surface, especially at the lower edges, then becoming negligible on the vertical surface. As a rule, with the exception of the vertical surface, the normal pressure is an order of magnitude higher than the friction stress. In the case of the higher piston speed, the

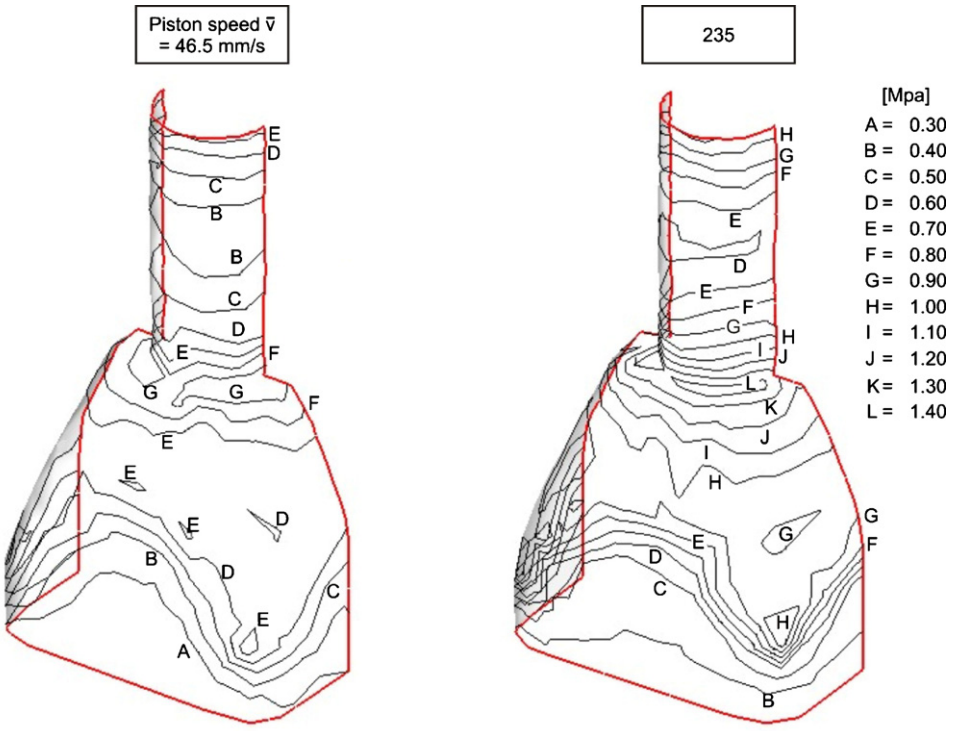

Fig. 11. von Mises equivalent stress of the clay on the surface of the die mandrel at various piston speeds.

normal pressure accounts for about two thirds of the force on the mandrel – the rest owing to friction –, whereas, for the lower piston speed, the contribution of normal pressure is only slightly greater than that of friction, as the lower strain rates affect pressure stronger (through the flow rule) than friction (through the Tresca law). While the sliding velocities on the mandrel surface are roughly proportional to the piston speed (the velocities for the 235 mm/s piston speed being about five times those for the 46.5 mm/s speed), the (normal and frictional) stresses are influenced in a lesser degree by the piston speed – they are about 1.5 times higher for the higher speed –, due to the form of the constitutive equation.

As shown in Fig. 11, the equivalent stress on the surface of the mandrel (to which the friction stress is proportional by the Tresca friction factor) rises only moderately with the extrusion speed, being more affected on the inclined surface, as the pressure on the vertical surface remains low even at high extrusion speeds.

6. Conclusions

The characteristic material parameters of the rigid–viscoplastic constitutive equation for the flow of wet clay during the extrusion of ceramic products were determined through comparison of the force–displacement curves obtained by a ram extrusion trial and its numerical simulation. The Tresca friction law applied to describe the contact between the plastically deforming clay and the rigid walls of the experimental device is well supported by the experimental results. The value of the Tresca friction factor m proved decisively important for the obtained results.

The numerical simulation of the flow has shown that no sticking areas appear between clay and die. As a result of the Tresca law and the form of the constitutive equation the significance of the friction stresses relative to that of the normal pressure is higher for lower extrusion speeds. However, at the extrusion speeds of the trials and particularly those applied in the production of ceramic products, which are close or higher than the higher speed tested here, the values of the normal pressure on the die mandrel are by an order of magnitude higher than those of the friction stress. The resulting equivalent stresses on the surface of the mandrel are quite low, in the order of magnitude of 1 MPa, indicating that wear of the mandrels occurs due to abrasion rather than mechanical load.

An important conclusion, which seems to hold for most simulations of viscoplastic flow, is the high impact of the applied friction boundary condition on the obtained results. Indeed, due to the generally high plastic flow consistency of viscoplastic materials, the flow pattern of the bulk material is not significantly affected by the friction on the walls. However, the assumed friction law strongly influences the calculated value of the extrusion force, owing to the usually considerable contribution of the friction stresses to the overall extrusion force. At high extrusion speeds, where the applied pressure on the material and consequently on the walls is high, the unrealistic application of the Coulomb friction law can result in an overestimation of the friction stresses and thus of the extrusion force, or in severely distorted estimates of the material parameters.

The developed methodology enables the determination of the superficial die loads during clay extrusion and thus of the stresses in hard coatings deposited on the dies.

Acknowledgement

The research was conducted in the frame of the "CERTO" Eureka project, supported by the General Secretariat of Research and Technology of the Hellenic Ministry for Development.

References

1. Adams, M. J., Aydin, I., Briscoe, B. J. and Sinha, S. K., A finite element analysis of the squeeze flow of an elasto-viscoplastic paste material. *J. Non-Newton. Fluid Mech.*, 1997, **71**, 41–57.
2. Aydin, I., Biglari, F. R., Briscoe, B. J., Lawrence, C. J. and Adams, M. J., Physical and numerical modeling of ram extrusion of paste materials: conical die entry case. *Comput. Mater. Sci.*, 2000, **18**, 141–155.
3. Basterfield, R. A., Lawrence, C. J. and Adams, M. J., On the interpretation of orifice extrusion data for viscoplastic materials. *Chem. Eng. Sci.*, 2005, **60**, 2599–2607.
4. Sherwood, J. D. and Durban, D., Squeeze flow of a power law viscoplastic solid. *J. Non-Newton. Fluid Mech.*, 1996, **62**, 35–54.
5. Sherwood, J. D. and Durban, D., Squeeze flow of a Hershel–Bulckley fluid. *J. Non-Newton. Fluid Mech.*, 1998, **77**, 115–121.
6. Alexandrov, S. and Richmond, O., Couette flows of rigid/plastic solids: analytical examples of the interaction of constitutive and frictional laws. *Int. J. Mech. Sci.*, 2000, **43**, 653–665.
7. Oezkan, N., Oysu, C., Briscoe, B. J. and Aydin, I., Rheological analysis of ceramic pastes. *J. Eur. Ceram. Soc.*, 1999, **19**, 2883–2891.
8. Ribeiro, M. J., Ferreira, J. M. and Labrincha, J. A., Plastic behaviour of different ceramic pastes processed by extrusion. *Ceram. Int.*, 2005, **31**, 515–519.
9. Franks, G. V. and Lange, F. F., Plastic clay-like flow stress of saturated advanced ceramic powder compacts. *J. Eur. Ceram. Soc.*, 2001, **21**, 893–899.
10. Ancey, C., Plasticity and geophysical flows: a review. *J. Non-Newton. Fluid Mech.*, 2007, **142**, 4–35.
11. Engmann, J., Servais, C. and Burbidge, A. S., Squeeze flow theory and applications to rheometry: a review. *J. Non-Newton. Fluid Mech.*, 2005, **132**, 1–27.
12. DEFORM 3D, Version 5 User's Manual, Scientific Forming Technologies Corporation, Columbus, OH, USA, 2004.
13. SOLIDWORKS User's Guide, Solidworks Corporation, Concord, MA, USA, 2006.
14. Kulikov, O. L. and Hornung, K., Wall detachment and high rate surface defects during extrusion of clay. *J. Non-Newton. Fluid Mech.*, 2002, **07**, 133–144.